Heat Treatment of Alumina Aerogels

Shani Keysar, Gennady E. Shter,* Yoram de Hazan, Yachin Cohen, and Gideon S. Grader

Chemical Engineering Department, Technion, Haifa 32000, Israel

Received April 10, 1997. Revised Manuscript Received September 15, 1997[⊗]

The phase conversions and morphological changes of alumina aerogel films and monoliths during heat treatment were investigated by TGA/DTA, BET, XRD, and image analysis of SEM micrographs. A preliminary model explaining the structural evolution of the film during heat treatment is proposed.

Introduction

Sol−gel processes have been used widely to obtain fibers, thin films, coatings and monoliths. Recently, using supercritical drying, we have obtained alumina aerogel monoliths and films[1,2] with high porosity and special morphology, different from those of common aerogels films.[3−4] The morphology of the films consists of fiberlike network of round chains (0.1 μm thick) and pores (0.1−0.5 μm in diameter). Formation of this microstructure was attributed to phase separation in the alumina−water−acetone system.[2] Related morphologies were cited in the literature for silica and titania films prepared by quite different techniques.[5−6]

One of the main questions concerning the application of these aerogels is their thermal stability. The structural evolution during heat treatment may be dominated by the effects of phase transformations that often occur along with dehydration.[7−8] There are several reports on the thermal treatment of alumina xerogels[9−12] that demonstrate that the thermal behavior depends on phase composition and morphological parameters of the starting material (degree of crystallinity, size of crystallites, porosity, etc.). Only a few studies follow the thermal behavior of alumina aerogels.[13−17] Mizushima and Hori[14−16] examined the influence of different synthesis routes on surface area, phase transition, and morphology properties of alumina aerogels. Ponthieu et al.[17] studied pure and yttrium-containing alumina aerogels. Little is known on the kinetics of sintering of gel films and particularly on films with this special morphology.[18,19]

The main goals of the present work were investigation of the phase conversions, morphological changes and thermal stability of the alumina aerogel monoliths and films, and the development of a preliminary model to explain the structural evolution of the films.

Experimental Section

The full details of monoliths/film preparation is discussed elsewhere.[1,2] Gel samples with different ratio of catalyst to aluminum *sec*-butoxide (ASB, Aldrich, purity 97%) in the range of 0.01−0.6 mol of H^+/mol of ASB (named groups a−d: a 0.01, b 0.07, c 0.2, d 0.6) were supercritically dried. The difference between the groups was that the pH of final sols before gelation was about 7 for group a, and in the range of 1−6 for groups b−d. Aerogel films were produced from sol b (which was found to be with the highest surface area after supercritical drying (SCD)[1,2]) on alumina substrates by exchanging the film solvent with acetone after the dip coating, followed by liquid CO_2 supercritical drying.[1,2] After SCD both monoliths and films were stored in sealed vials in a desiccator under vacuum at room temperature. Simultaneous thermogravimetric and differential thermal analysis (TGA/DTA) was performed on alumina monoliths at a heating rate of 5 °C/min up to 1300 °C under flowing air/argon using Setaram TGA-92 analyzer. Heat treatment of films on alumina substrates was done in air by the following thermal profile: a slow heating step (70 °C h^{-1} up to 400 °C), a faster step (200 °C h^{-1} up to 800−1300 °C), a soak at the high temperature for an hour, and finally cooling at 250 °C h^{-1} to room temperature. All TGA/DTA and heat-treatment experiments were repeated at least twice. Surface areas of the aerogels were determined by the single-point Brunauer, Emmet, and Teller (BET) method by nitrogen adsorption at 77 K using Micromeritics, Flowsorb II-2300. X-ray diffraction (XRD) Cu Kα radiation was done using a Siemens 5000 instrument. SEM micrographs were taken with a JEOL-5400. Image analysis was performed on a Power-Macintosh Model 6100 computer, with the public domain NIH Image software (written by Wayne Rasband at the US National Institute of Health (NIH)).

Results and Discussion

Thermal Treatment of Monoliths. Before any heat treatment, boehmite was identified in the bulk

[⊗] Abstract published in *Advance ACS Abstracts,* November 1, 1997.

(1) Keysar, S.; de Hazan Y.; Cohen Y.; Aboud T.; Grader, G. S. *J. Mater. Res.* **1997**, *12*, 430.
(2) Grader, G. S.; Rifkin, Y.; Cohen, Y.; Keysar, S. Presented at the 8th International Workshop on Glass and Ceramics from Gels, Portugal, **1995**. *J. Sol-Gel Sci. Technol.* **1997**, *8*, 197.
(3) Prakash, S. S.; Brinker, C. J.; Hurd, A. J.; Rao, S. M. *Nature* **1995**, *374*, 439.
(4) Hrubesh, L. W.; Poco, J. F. *J. Non-Cryst. Solids* **1995**, *188*, 46.
(5) El-Shall, M. S.; Li, S.; Turkki, T.; Graiver, D.; Pernisz, U. C.; Baraton, M. I. *J. Phys. Chem.* **1995**, *99*, 17805.
(6) Kim, Y. J.; Francis, L. F. *J. Am. Ceram. Soc.* **1993**, *76*, 737.
(7) Rama Rao, G. V.; Venkadesan, S.; Saraswati, V. *J. Non-Cryst. Solids* **1989**, *111*, 103.
(8) Balek, V.; Klosova, E.; Murat, M.; Camargo, N. A. *Am. Ceram. Bull.* **1996**, *75*, 73.
(9) Colomban, Ph.; Vendange, V. *J. Non-Cryst. Solids* **1992**, *147−148*, 245.
(10) Yoldas, B. E. *J. Mater. Sci.* **1975**, *10*, 1856.
(11) Yoldas, B. E. *J. Am. Ceram. Soc.* **1982**, *65*, 387.
(12) Wilson, S. J.; Stacey, M. H. *J. Colloid Interface Sci.* **1980**, *82*, 507.
(13) Teichner, S. J.; Nicolaon, G. A.; Vicarini, M. A.; Grades, G. E. E. *Adv. Colloid Interface Sci.* **1976**, *5*, 245.
(14) Mizushima, Y.; Hori, M. *J. Mater. Res. Soc.* **1993**, *8*, 2993.
(15) Mizushima, Y.; Hori, M. *J. Non-Cryst. Solids* **1994**, *167*, 1.
(16) Mizushima, Y.; Hori, M. *J. Eur. Ceram. Soc.* **1994**, *14*, 117.
(17) Ponthieu, E.; Grimblot, J.; Elaloui, E.; Pajonk, G. M. *J. Mater. Chem.* **1993**, *3*, 287.
(18) Brinker, C. J.; Scherer, G. W. *Sol−Gel Science: The Physics and Chemistry of Sol−Gel Processing;* Academic Press Inc.: New York, 1990.
(19) Scherer, G. W.; Garino, T. *J. Am. Ceram. Soc.* **1985**, *68*, 216.

S0897-4756(97)00208-1 CCC: $14.00

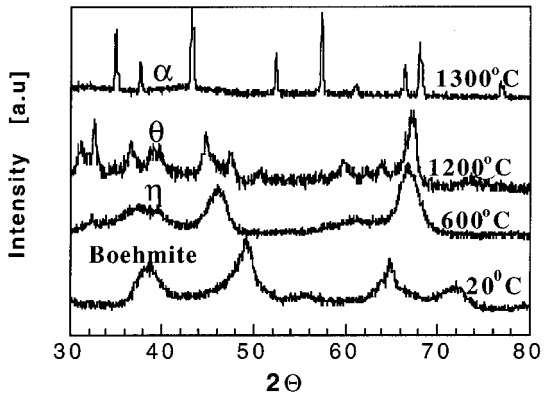

Figure 1. Effect of heat treatment on phase transformation of alumina aerogel (group b, 0.07 mol of H^+/mol of Al).

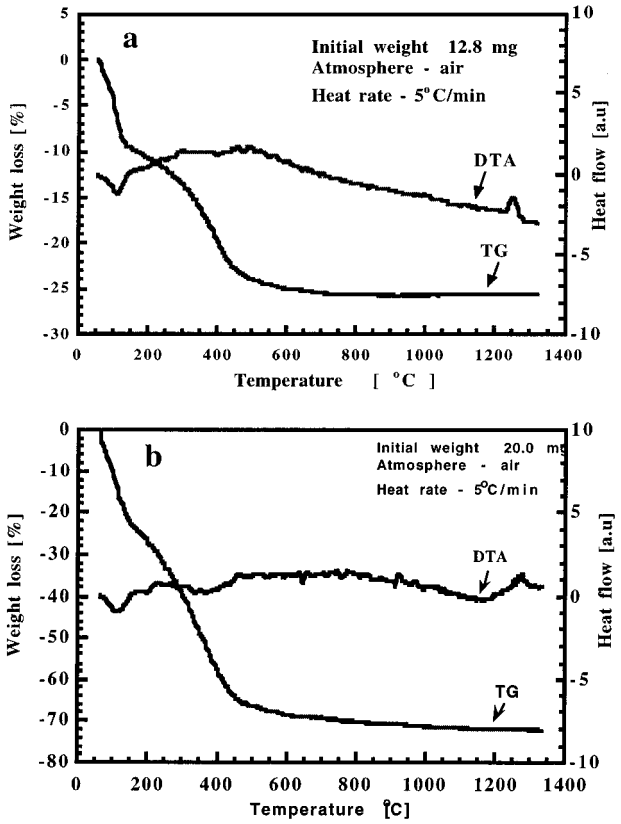

Figure 2. TGA/DTA of alumina aerogel monoliths (a) group a, 0.01 mol of H^+/mol of Al and (b) group b, 0.07 mol of H^+/mol of Al.

samples of all aerogels. This is shown in the lower diffractogram in Figure 1, where data for group b are presented.

The TGA/DTA data of monoliths of group a are presented in Figure 2a, while typical data of groups b−d are seen in Figure 2b. The thermogram profiles of all groups could be divided into three main regions: (1) 20−150 °C, (2) 150−600 °C, and (3) 600−1300 °C, that are in general also typical to the thermal behavior of xerogels.[7−12]

The first region (see Figure 2) is characterized by an endo effect at 70−130 °C attributed to evolution of physically adsorbed water accompanied with calculated weight loss of 7−12%. The calculation of weight loss on the next regions was normalized to the weight of samples free from desorbed water.

The second region (see Figure 2) includes the boehmite−alumina conversion and presented on the thermograms by a weak endo effect in a wide temperature range of 150−600 °C accompanied with a weight loss of 15−28%. This weight loss is a result of the following reactions:

$$2AlOOH \rightarrow Al_2O_3 + H_2O \quad \text{for group a} \qquad (1)$$

theoretical weight loss 17.7

$$2AlOOH \cdot 1.7H_2O \rightarrow Al_2O_3 + 2.7H_2O \quad \text{for groups b−d} \qquad (2)$$

theoretical weight loss 26.8%.

Experimental weight loss for group a was 17% and for groups b−d 24.1−26.1%. Thus, although XRD for all groups is similar, from TGA data we found a significant difference between aerogel group a (prepared at the lowest H^+/ASB ratio (0.01)), and groups b−d: aerogel a is boehmite and the rest are pseudoboehmite. The existence of boehmite and pseudoboehmite of alumina xerogels is also known to be depended on the pH during gelation. Below pH = 3 Al^{3+} has a coordination number of 6, with increasing pH the coordination number decreases.[18,20]

We suggest that the higher coordination number allows the formation of the phase with larger amount of chemically bonded water. Therefore the more acidic gels groups b−d included the pseudoboehmite phase. XRD data of all aerogels heated at 600 °C (Figure 1) shows that the final phase obtained by the above conversions (eq 1,2) is η-Al_2O_3 identified according to ref 21.

The third region (~600−1300 °C) seen in Figures 2 includes phase transitions η/θ and θ/α of alumina accompanied by negligible weight loss. Only the θ/α-Al_2O_3 is followed by exopeak at ~1220−1240 °C seen on the thermograms (Figure 2). XRD data show that the main phases in the ranges of 600−1100 and 1100−1200 °C are η-Al_2O_3 and θ-Al_2O_3, respectively (Figure 1). In conclusion, the conversions of the prepared alumina aerogels under heat treatment can be summarized as follows:

$$\text{(group a) boehmite} \rightarrow \eta \rightarrow \theta \rightarrow \alpha\text{-}Al_2O_3$$

$$\text{(groups b−d) pseudoboehmite} \rightarrow \eta \rightarrow \theta \rightarrow \alpha\text{-}Al_2O_3 \qquad (3)$$

BET measurements (see Figure 3) show that up to ~800 °C the surface area (SA) of monoliths remained ~350 m^2/g. During this stage the change of SA observed can be a result of two possible opposite phenomena. On one hand, dehydration of hydroxides promotes shrinkage (due to increase of tension in the pores) and as a result a decrease in surface area. On the other hand, condensation of protons and hydroxyls between boehmite layers removes half of the oxygens from the layers causing rearrangement and leading to the phase conversion boehmite/η-Al_2O_3 (spinel structure). The phase conversion is followed by a decrease in the size of the

(20) Yoldas, B. E. *J. Mater. Sci.* **1975**, *10*, 1856.
(21) Wefers, K.; Misza, C. *Oxides and Hydroxides of Aluminum;* Alcoa Laboratories; 1987.

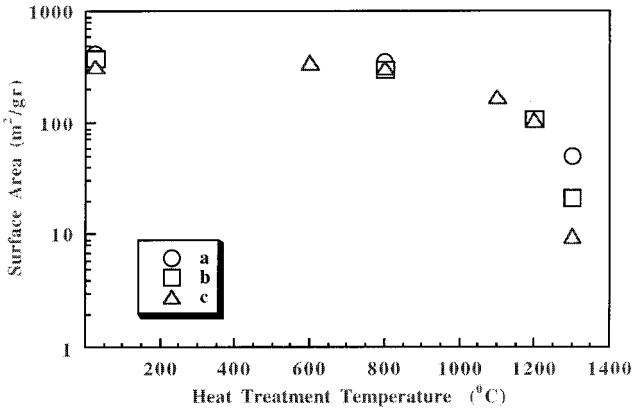

Figure 3. Surface area of heat treated alumina aerogels (group a, 0.01; b, 0.07; c, 0.2 mol of H^+/mol of Al).

crystallites and a corresponding increase in SA. This phenomenon has been observed earlier for boehmite/γ-Al_2O_3 conversion in xerogels.[22] Consequently the surface area changes are small. From ~800 °C to ~1100 °C, according to XRD η-Al_2O_3 is identified, and SA decreases to ~180 m^2/g. Within the interval ~1100−1220 °C η/θ phase transition occurs along with the loss of transparency and SA decreases to ~100 m^2/g. Finally, above 1220 °C θ/α transition is indicated by TGA/DTA and XRD. This transition involves a reorganization of the oxygens into a denser, hexagonal close-packed configuration by a nucleation-and-growth process.[23] As a result a drastic fall of the SA to a low level of ~10−40 m^2/g is noticed. Although the pH affects the SA of the starting materials,[1] it does not influence their behavior under heat treatment up to about 1200 °C. However, after the transition to α-Al_2O_3, the lower pH aerogels maintain much higher SA. The influence of the pH at the gel point on the aerogels thermal stability, needs further research.

Thermal Treatment of Films. Aerogels films were synthesized from sol b, which was found to have the highest SA after supercritical drying.[1] Although the pH and BET measurements were carried out on bulk monolithic samples. Due to experimental difficulties, these measurements could not be repeated with the dip-coated film samples. However, TEM micrographs of film and bulk samples (from sol b) reveals that the nanostructure is identical in both cases.[1,2] Since the phase transition occurs at the nanoscale level, we believe that XRD results represents both bulk and film samples. The fiberlike morphology of the films retained up to ~1000 °C (see Figure 4a−c). The average macroporosity of the films estimated by image analysis is around 50%. Figure 4d describes the changes in the surface porosity of the films. The deformation of a thin film is usually constrained by a substrate.[18,19] In our case the increase of surface porosity as measured by the image analysis of SEM micrographs at low temperatures is most likely due to a decrease of the fiber radius accompanying the dehydration of hydroxides. At this temperatures no decrease of the overall film dimensions is observed, thus as a first approximation, the dependence of the surface porosity on fiber diameter is given by the relation below (see Figure 5):

$$P = 1 - \bar{l}r/S \tag{4}$$

where P is the surface porosity, S is a representative arbitrary area, and r and $\bar{l}$ are the average fiber radius and the overall fiber network length measured at S respectively (r and $\bar{l}$ are shown in Figure 5). Regarding the fiber network as consisting of spherical particles (0.1 μm in diameter) requires that $\bar{l} \propto r^I$ through the densification process, where I is defined as an isotropic shrinkage factor, $0 \le I \le 1$. Equation 4 then becomes

$$P = 1 - Kr^I r/S \tag{5}$$

where K is a proportionality constant. In this development we assume that anisotropy can occur only along the $\bar{l}$ axis. Moreover, we assume similar shrinkage mechanisms in the free fiber and at the fiber intersections. The change in surface porosity with respect to variations in fiber radius is then directly obtained from

$$\left(\frac{1-P}{1-P_0}\right)^{1/1+I} = \left(\frac{r}{r_0}\right) \tag{6}$$

where P_0 and r_0 are the initial parameters of the film. Isotropic shrinkage of the particles is expected if the fiber network is flexible enough to decrease its length and curvature in order to decrease the axial strain developed during the shrinkage process. In this case $\bar{l} \propto r$ and $I = 1$. However, if the fiber network constrained between the intersections does not have enough mobility, the axial strain would cause the spherical particles to deform and to shrink anisotropically. At the extreme condition of completely anisotropic shrinkage $\bar{l}$ is essentially unchanged through the densification process and $I = 0$. Taking the surface porosity values of 0.48 at 25 °C and 0.62 at 800 °C (Figure 4d), we obtain the ratios $r/r_0 = 0.86$ and $r/r_0 = 0.73$ for the isotropic and anisotropic cases, respectively. The predicted shrinkage of 14−27% in fiber radius cannot be observed by our image analysis technique. This result reinforces our observation that in this stage of thermal treatment a decrease of the fiber radius occurs accompanying the dehydration of hydroxides. Titanium films with similar morphology also maintained their open structure without significant change after heat treatment up to ~850 °C.[5,6]

At the high-temperature interval, shrinkage of the films and drastic changes in the density of the network occur. Here the shrinkage occurs in the plane of the substrate. It is interesting to compare our results with Scherer's[19] model for a viscous porous film where a layer is represented by tubes with their axes normal to the substrate. His model predicts a shrinkage in the plane tangent to the surface and a decrease in the inner diameter of the tube in the case of anisotropic sintering. His results are generally in agreement with the behavior of the film in the high-temperature region.

Conclusions

The phase conversions, morphological changes, and thermal stability of alumina aerogels during heat treatment were investigated. The initial neutral and acidic bulk aerogels were identified as boehmite and pseudoboehmite, respectively. The phase conversions in the

(22) Zacharchenya, R. I.; Vasilevskaya, T. N. *Zur. Prikl. Chim.* **1992**, *65*, 2707.
(23) Kumagai, M.; Messing, G. L. *J. Am. Ceram. Soc.* **1985**, *68*, 500.

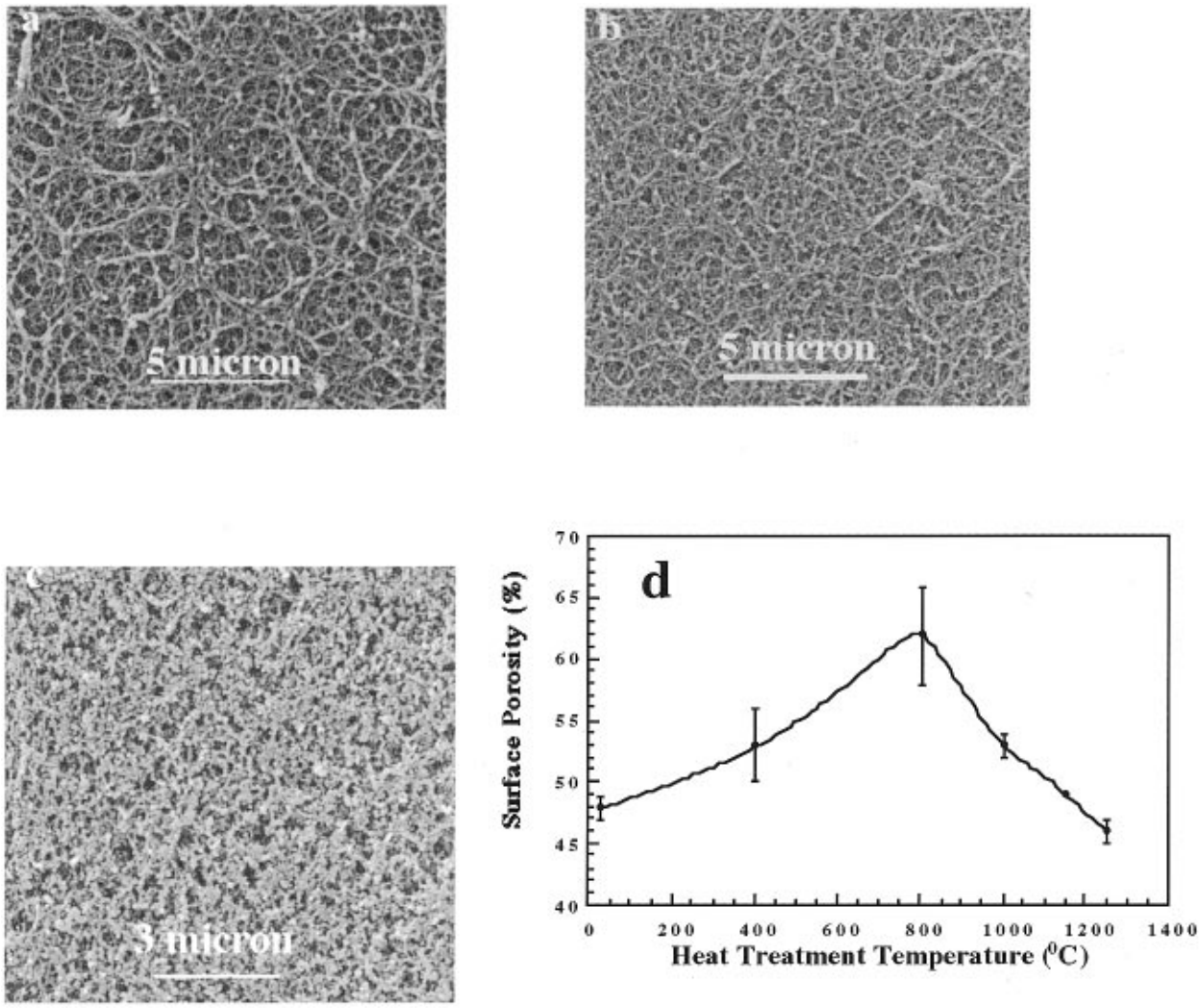

Figure 4. Effect of heat treatment on alumina aerogel film morphology: (a) before treatment, (b) after 800 °C, (c) after 1250 °C, and (d) evolution of surface area porosity from image analysis.

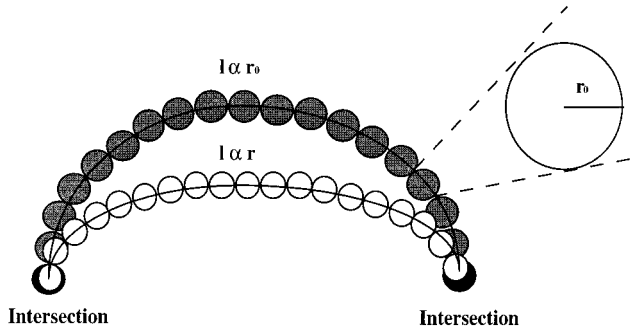

Figure 5. Film model parameters.

range 20−1300 °C were as follows: boehmite/pseudo-boehmite → η-Al_2O_3 → θ-Al_2O_3 → α-Al_2O_3. Up to ∼800 °C the surface area (SA) of monoliths remained ∼350 m^2/g. From ∼800 to ∼1100 °C, we observed η-Al_2O_3 by XRD, and SA decreased to ∼180 m^2/g. Within the interval ∼1100−1220 °C the η/θ phase transition along with particle growth occurred and SA dropped to ∼100 m^2/g. Finally, above 1220 °C θ/α occurs and as a result a drastic fall of the SA to a low level of ∼10−40 m^2/g was noticed. The decrease of SA of monoliths was shown to depend on the combined effect of dehydration and condensation. Although the pH effects the SA of the starting materials,[1] it does not influence their behavior under heat treatment up to about 1200 °C; however, after the transition to α-Al_2O_3 the lower pH aerogels maintain much higher SA.

The unique initial morphology of the films as well-the transparency of the monoliths were retained up to ∼1000 °C. A geometrical model was developed to explain the structural evolution of the film during the early stages of heat treatment.

Acknowledgment. This work was supported by the Israeli Ministry of Science and the Fund for Promotion of Research at the Technion.

CM970208S